

## Observations and light curve solutions of the W UMa binaries V796 Cep, V797 Cep, CSS J015341.9+381641 and NSVS 3853195

D. P. Kjurkchieva<sup>1</sup>, V. A. Popov<sup>1,2</sup>, S. I. Ibryamov<sup>1</sup>, D. L. Vasileva<sup>1</sup>, N. I. Petrov<sup>3</sup>

<sup>1</sup> Department of Physics, Shumen University, 115 Universitetska Str., 9712 Shumen, Bulgaria;  
*d.kjurkchieva@shu.bg*

<sup>2</sup> IRIDA Observatory, Rozhen NAO, Bulgaria

<sup>3</sup> Institute of Astronomy and NAO, Bulgarian Academy of Sciences, 72 Tsarigradsko Shose Blvd., 1784  
Sofia, Bulgaria

Received ; ccepted

**Abstract** Photometric observations in Sloan  $g'$  and  $i'$  bands of four W UMa binaries, V796 Cep, V797 Cep, CSS J015341.9+381641 and NSVS 3853195, are presented. Our observations showed that CSS J015404.1+382805 and NSVS 3853195 are the same star. We determined the initial epochs  $T_0$  of all targets and improved the period of NSVS 3853195. The light curve solutions of our data revealed that the components of each target are almost the same in mass, temperature, radius and luminosity. The stellar components are of G and K spectral types and undergo partial eclipses. All systems have barely-overcontact configurations and belong to H subtype W UMa binaries. We established that the relation between the luminosity ratio  $l_2/l_1$  and mass ratio  $q$  of our targets is approximately  $l_2/l_1 = q^{1.5}$ .

**Key words:** stars: binaries: eclipsing; stars – fundamental parameters; stars – individual (V796 Cep, V797 Cep, CSS J015341.9+381641, NSVS 3853195)

## 1 INTRODUCTION

The creation of stellar evolutionary scheme requires a knowledge of the fundamental parameters of stars in different stages of their evolution. Eclipsing binary systems, especially W UMa binaries, are the most important sources of such information. It is supposed that they are result from the evolution of wide binaries by angular momentum loss and mass-ratio reversals (Stepien 2006, Qian 2003). Around 25 % of main-sequence star binaries have separations small enough so when their primaries ascend the giant branch, mass transfer via Roche-lobe overflow puts the beginning of a common envelope phase (Willems & Kolb 2004). At this stage the two stars orbit within a single envelope of material, quickly losing angular momentum and spiraling towards each other (Webbink 1984; Ivanova et al. 2013). The common-envelope phase is probably a short-lived stage that ends by envelope ejection and a tighter binary or by a merger. But understanding of common envelope stage remains one of the most important unsolved problems in stellar evolution (Ivanova et al. 2013).

The components in a W UMa system have nearly equal surface temperatures in spite of their often greatly different masses (Binnendijk 1965). The model of Lucy (1968b), Lucy (1968a) explained this effect by a common convective photosphere which embedded two main sequence stars. As a result one should expect the observable luminosities to have another dependence on the mass ratio than would be the case of two main sequence stars in detached configuration. The condition for equal surface temperatures leads to specific period-luminosity-color (PLC) relations of W UMa stars (Rucinski 1994, Rucinski & Duerbeck 1997) allowing currently to predict their absolute magnitudes  $M_V$  to about 0.25 mag (Rucinski 2004). The PLC relations combined with the ease detection make these binaries useful tracers of distance (Klagyivik & Csizmadia 2004; Gettel et al. 2006; Eker et al. 2009). Moreover, the W UMa stars are important targets for the modern astrophysics because they give information for the processes of tidal interactions, mass loss and mass transfer, angular momentum loss, merging or fusion of the stars (Martin et al. 2011).

In this paper we present photometric observations and light curve solutions of four W UMa binaries: V796 Cep (GSC 04502-00138, TYC 4502-138-1), V797 Cep (GSC 04502-01040, 2MASS J01424764+8007522), CSS J015341.9+381641, NSVS 3853195 (CSS J015404.1+382805). Table 1 presents the coordinates of our targets and available information for their light variability.

**Table 1** Parameters of our targets from the VSX database

Target	RA	Dec	Period [d]	V [mag]	Amplitude [mag]	Type
V796 Cep	01 41 36.39	+80 04 19.1	0.3929661	12.20	0.65	EW
V797 Cep	01 42 47.64	+80 07 52.3	0.270416	14.60	0.40	EW
CSS J015341.9+381641	01 53 41.95	+38 16 41.1	0.347518	13.47	0.40	EW
NSVS 3853195	01 54 04.05	+38 28 05.2	0.29253	13.52	0.39	EW

**Table 2** Journal of our photometric observations

Target	Date	Exposure $g'$	Exposure $i'$	Number $g'$	Number $i'$
V796 Cep, V797 Cep	2015 Oct 25	90	120	125	125
	2015 Oct 26	90	120	84	82
	2015 Oct 27	90	120	60	59
	2015 Oct 28	90	120	146	146
CSS J015341.9+381641, NSVS 3853195	2015 Nov 07	60	90	85	84
	2015 Nov 08	60	90	67	75
	2015 Nov 11	60	90	84	84
	2015 Nov 12	60	90	43	42
	2015 Nov 13	60	90	84	85

## 2 OBSERVATIONS

Our CCD photometric observations of the targets in Sloan  $g'$ ,  $i'$  bands were carried out at Rozhen National Astronomical Observatory with the 30-cm Ritchey-Chrétien Astrograph (located into the *IRIDA South* dome) using CCD camera ATIK 4000M ( $2048 \times 2048$  pixels,  $7.4 \mu\text{m}/\text{pixel}$ , field of view  $35 \times 35$  arcmin). Information for our observations is presented in Table 2. In fact, the pairs V796 Cep, V797 Cep and CSS J015341.9+381641, NSVS 3853195 fall on two observed fields (see coordinates in Table 1).

The data were obtained during photometric nights with seeing within 1.1–1.9 arcsec and humidity below 70 %. Twilight flat fields were obtained for each filter, dark and bias frames were also taken throughout the run. The frames were combined respectively into a single master bias, dark and flat frames. The standard procedure was used for reduction of the photometric data (de-biasing, dark frame subtraction and flat-fielding) by software AIP4WIN2.0 (Berry & Burnell 2006).

**Table 3** List of the standard stars

Label	Star ID	RA	Dec	$g'$	$i'$
Target 1	V0796 Cep	01 41 36.39	+80 04 19.10	12.320	11.789
Target 2	V0797 Cep	01 42 47.64	+80 07 52.30	14.966	14.025
Chk	UCAC4 851-002007	01 41 16.52	+80 04 21.76	13.755 (0.010)	13.018 (0.010)
C1	UCAC4 851-002085	01 45 07.01	+80 10 45.03	13.238 (0.011)	12.534 (0.011)
C2	UCAC4 851-002011	01 41 28.03	+80 11 18.42	13.870 (0.010)	13.351 (0.012)
C3	UCAC4 851-002002	01 40 56.97	+80 04 14.51	13.448 (0.009)	12.844 (0.010)
C4	UCAC4 851-002062	01 43 56.73	+80 02 08.49	14.205 (0.011)	13.452 (0.013)
C5	UCAC4 850-002063	01 41 51.38	+79 56 58.55	13.257 (0.007)	12.651 (0.009)
C6	UCAC4 851-002028	01 42 25.41	+80 01 00.68	13.898 (0.009)	13.058 (0.009)
Target 3	CSS J015341.9+381641	01 53 41.95	+38 16 41.10	13.897	13.117
Target 4	NSVS 3853195	01 54 04.05	+38 28 05.26	14.054	13.178
Chk	UCAC4 643-007188	01 54 30.68	+38 29 00.15	13.104 (0.014)	11.754 (0.009)
C1	UCAC4 644-007104	01 54 12.54	+38 36 49.06	13.975 (0.016)	13.902 (0.018)
C2	UCAC4 643-007165	01 54 04.61	+38 35 54.88	14.112 (0.011)	13.419 (0.015)
C3	UCAC4 643-007180	01 54 23.95	+38 35 42.60	14.061 (0.014)	13.369 (0.015)
C4	UCAC4 643-007204	01 54 50.23	+38 33 52.57	13.971 (0.019)	13.147 (0.015)
C5	UCAC4 643-007182	01 54 26.03	+38 29 38.62	13.720 (0.009)	13.012 (0.011)
C6	UCAC4 643-007126	01 53 26.47	+38 30 02.18	13.702 (0.016)	12.978 (0.013)
C7	UCAC4 642-006881	01 54 12.52	+38 23 56.10	13.937 (0.012)	12.907 (0.011)
C8	UCAC4 642-006842	01 53 30.38	+38 20 34.86	13.929 (0.024)	13.071 (0.018)
C9	UCAC4 642-006908	01 54 36.06	+38 20 04.67	14.068 (0.013)	11.491 (0.014)
C10	UCAC4 642-006921	01 54 46.30	+38 19 35.13	13.161 (0.021)	11.764 (0.014)
C11	UCAC4 643-007147	01 53 51.89	+38 28 10.11	12.849 (0.018)	12.191 (0.014)

We used aperture photometry with radius of 1.5 FWHM of the star image, along with sky background measurements with annuli enclosing a comparable area. The light variability of the targets was estimated with respect to nearby comparison (constant) stars in the observed field of each target, so called ensemble photometry. A check star served to determine the observational accuracy and to check constancy of the comparison stars. The CCD ensemble photometry calculates the difference between the instrumental magnitude of the target and a comparison magnitude obtained from the mean of the intensities of the comparison stars. The use of numerous comparison stars scattered over the CCD field increases considerably the statistical accuracy of the comparison magnitude (Gilliland & Brown 1988, Honeycutt 1992).

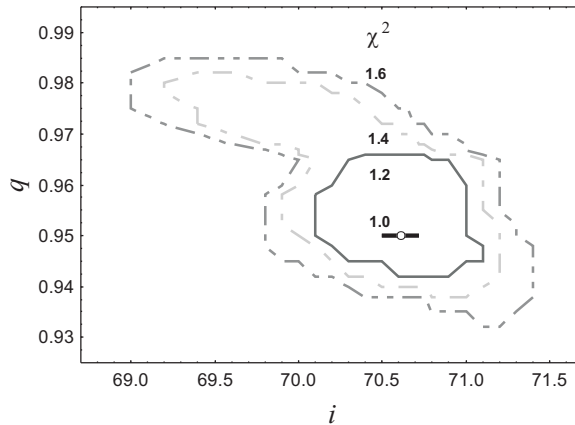


**Fig. 1** Illustration of the  $q$ -search analysis for V796 Cep: the different isolines circumscribe the areas whose normalized  $\chi^2$  are smaller than the marked values; the empty circle corresponds to the final value of the mass ratio and orbital inclination given in Table 5.

We performed the ensemble aperture photometry with the software VPHOT. Table 3 presents the coordinates of the comparison and check stars of our targets from the catalogue UCAC4 (Zacharias et al. 2013) and their magnitudes from the catalogue APASS DR9 (Henden 2016). The values in brackets correspond to the standard deviations of the standard stars during the observational nights. The choice of comparison and check stars in the same field of view of the targets means practically equal extinctions for all stars. The transformation of the obtained instrumental magnitudes to standard ones was made manually. For this aim we used the mean color of the ensemble comparison-star  $\overline{(g' - i')_{comp}}$  and transformation coefficients of our equipment (calculated earlier using standard star field M67). The calculated corrections of the instrumental magnitudes for our targets were from  $-0.0008$  mag to  $0.0003$  mag in  $g'$  filter (within the observational precision) and from  $-0.0258$  mag to  $0.0085$  mag in  $i'$  filter.

We determined the times of the individual minima (Table 4) by the method of Kwee & van Woerden (1956).

### 3 LIGHT CURVE SOLUTIONS

The light curves of our targets were solved by the code PHOEBE (Prsa & Zwitter 2005). It is based on the Wilson–Devinney (WD) code (Wilson & Devinney 1971, Wilson 1979) but also provides a graphical user

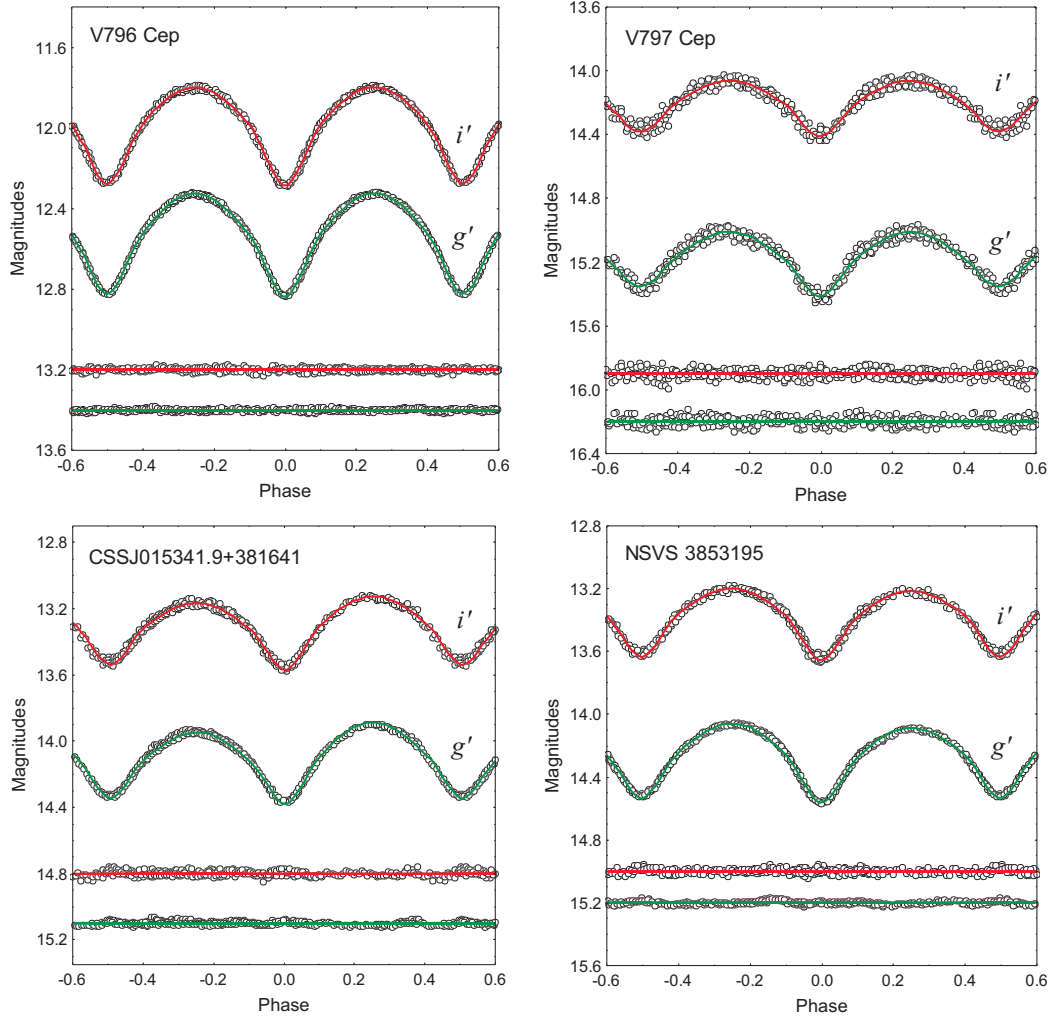


**Fig. 2** The folded light curves of the targets with their fits and the corresponding residuals (shifted vertically by different amount to save space).

interface and modeling in Sloan filters of our observations. We used the traditional convention the Min. I (phase 0.0) to be the deeper light minimum and the star that is eclipsed at Min. I to be a primary component.

Mean temperatures  $T_m$  of the binaries were determined in advance (see Table 6 further) on the basis of their infrared color indices ( $J-K$ ) from the 2MASS catalog and the calibration color-temperature of Tokunaga (2000). The preliminary runs revealed that all targets are overcontact systems. Hence, we applied mode

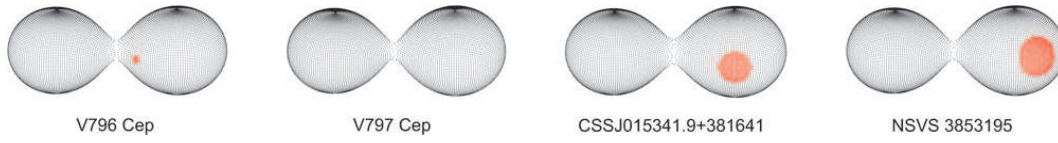


**Fig. 3** 3D configurations of the targets

**Table 4** Times of minima of our targets

Target	Min. I	Min. II	IRIDA cycle
V0796 Cep	2457321.43582(9)	-	0.0
	-	22457322.41776(13)	2.5
	2457323.40045(19)	-	5.0
	-	2457324.38263(8)	7.5
	2457324.57929(1)	-	8.0
V0797 Cep	2457321.31715(74)	-	0.0
	-	2457321.45201(25)	0.5
	2457321.58629(22)	-	1.0
	-	2457322.26135(33)	3.5
	2457322.39815(24)	-	4.0
	-	2457323.34511(22)	7.5
	2457324.29034(18)	-	11.0
CSS J015341.9+381641	-	2457333.44320(11)	-0.5
	2457333.61496(31)	-	0.0
	-	2457334.48599(14)	2.5
	2457338.47982(18)	-	14.0
	-	2457340.39396(31)	19.5
	2457340.56578(15)	-	20.0
NSVS 3853195	-	2457333.44266(9)	-0.5
	2457333.59001(21)	-	0.0
	2457334.46774(15)	-	3.0
	-	2457338.41610(11)	16.5
	2457338.56296(13)	-	17.0
	2457339.44062(12)	-	20.0
	-	2457340.46366(14)	23.5

”Overcontact binary not in thermal contact” of the code. Firstly we fixed  $T_1 = T_m$  and varied the initial epoch  $T_0$  and period  $P$  to search for fitting the phases of light minima and maxima. After that we fixed their values and varied simultaneously secondary temperature  $T_2$ , orbital inclination  $i$ , mass ratio  $q$  and potential  $\Omega$  to search for reproducing of the whole light curves. The data in  $i'$  and  $g'$  bands were modelled simultaneously.

We adopted coefficients of gravity brightening  $g_1 = g_2 = 0.32$  and reflection effect  $A_1 = A_2 = 0.5$  appropriate for late-type stars while the linear limb-darkening coefficients for each component and each color were updated according to the tables of [van Hamme \(1993\)](#). Solar metallicity was assumed for the targets because they consist of late stars from the solar vicinity. In order to reproduce the light curve distortions we used cool spots whose parameters (longitude  $\lambda$ , angular size  $\alpha$  and temperature factor  $\kappa$ ) were adjusted.

After reaching the best solution we varied together all parameters ( $T_2$ ,  $i$ ,  $q$ ,  $\Omega$ ,  $T_0$  and  $P$ ) around the values from the last run and obtained the final model. In order to determine stellar temperatures  $T_1$  and  $T_2$  around the mean value  $T_m$  we used the formulae ([Kjurkchieva et al. 2016b](#)):

$$T_1 = T_m + \frac{\Delta T}{c + 1}, \quad (1)$$

$$T_2 = T_1 - \Delta T, \quad (2)$$

where  $c = l_2/l_1$  (luminosity ratio) and  $\Delta T = T_m - T_2^{PH}$  were taken from the last PHOEBE fitting.

Although PHOEBE (as WD) works with potentials, it gives a possibility to calculate all values (polar, point, side, and back) of relative radius  $r_i = R_i/a$  of each component ( $R_i$  is linear radius and  $a$  is orbital separation). In the absence of radial velocity curves we put as default  $a = 1$  because from photometry only we cannot determine binary separation. Moreover, PHOEBE yields as output parameters bolometric magnitudes  $M_{bol}^i$  of the two components in conditional units (when radial velocity data are not available). But their difference  $M_{bol}^2 - M_{bol}^1$  determines the true luminosity ratio  $c = L_2/L_1 = l_2/l_1$ . Fillout factor  $f = [\Omega - \Omega(L_1)]/[\Omega(L_2) - \Omega(L_1)]$  can be also calculated from the output parameters of PHOEBE solution.

In order to take into account the effect of expected correlation between the mass ratio and orbital inclination we carried out  $q$ -search analysis as described in [Kjurkchieva et al. \(2016b\)](#). For this aim we fixed the component temperatures and radii as well as the spot parameters and calculated the normalized  $\chi^2$  for a two-dimensional grid along  $i$  and  $q$ . Figure 1 illustrates the result from this  $q$ -search procedure for the target V796 Cep.

Table 5 contains final values of the fitted stellar parameters and their PHOEBE uncertainties: initial epoch  $T_0$ ; period  $P$ ; mass ratio  $q$ ; inclination  $i$ ; potential  $\Omega$ ; secondary temperature  $T_2^{PH}$ . Table 6 exhibits

**Table 5** Values of the fitted parameters

Star	$T_0$	$P$	$q$	$i$	$\Omega$	$T_2^{PH}$
V796 Cep	2457321.43582(9)	0.392966	0.948(2)	70.7(1)	3.612(7)	6400(19)
V797 Cep	2457321.31715(74)	0.270416	0.886(2)	64.7(1)	3.525(2)	4625(42)
CSS J015341.9+381641	2457333.61496(31)	0.347518	0.892(2)	70.0(2)	3.490(1)	5607(28)
NSVS 3853195	2457333.59001(21)	0.292524(4)	0.899(2)	69.8(1)	3.539(3)	5592(30)

**Table 6** Calculated parameters

Target	$T_m$	$T_1$	$T_2$	$r_1$	$r_2$	$f$	$l_2/l_1$
V796 Cep	6407	6410(19)	6403(19)	0.421(1)	0.412(1)	0.101	0.951
V797 Cep	4770	4833(44)	4688(42)	0.424(1)	0.403(1)	0.075	0.771
CSS J015341.9+381641	5715	5765(29)	5657(28)	0.434(1)	0.414(1)	0.166	0.867
NSVS 3853195	5688	5733(31)	5637(30)	0.425(1)	0.406(1)	0.089	0.865

**Table 7** Parameters of the cool spots of the targets

Star	$\beta$	$\lambda$	$\alpha$	$k$
V796 Cep	90(5)	35(1)	5.0(1)	0.90(1)
CSS J015341.9+381641	90(5)	90(1)	20.0(1)	0.80(1)
NSVS 3853195	80(5)	120(1)	25.0(2)	0.95(1)

the calculated parameters: stellar temperatures  $T_{1,2}$ ; stellar radii  $r_{1,2}$  (back values); fillout factor  $f$ ; ratio of relative stellar luminosities  $l_2/l_1$ . Their errors are determined from the uncertainties of output parameters used for their calculation. Table 7 gives information for the spot parameters. The synthetic light curves corresponding to our solutions are shown in Fig. 2 as continuous lines.

The mean ( $g'$ ,  $i'$ ) residuals for the final fittings are: (0.005, 0.007) for V796 Cep; (0.021, 0.022) for V797 Cep; (0.009, 0.012) for CSS J015341.9+381641; (0.009, 0.013) for NSVS 3853195. The mean ( $g'$ ,  $i'$ ) residuals of the standard stars (Table 3) for the first and second pairs of targets are correspondingly (0.010, 0.011) and (0.017, 0.015). Hence, our fittings are excellent for the three targets and very good for the faint star V797 Cep (Fig. 2). The small imperfectness of our modeling may due to inadequate treatment of the overcontact binaries (Prsa et al. 2016) and to long exposures (Kipping 2010).

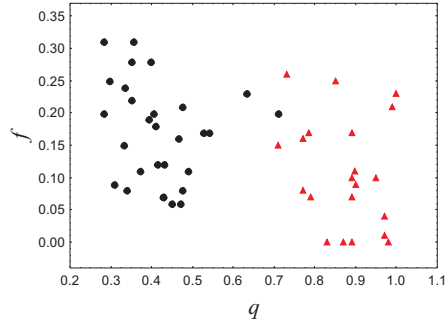


**Fig. 4** Distribution fillout factor– mass ratio of W UMa stars: red triangles are for shallow contact high mass ratio targets; black circles are for targets with decreasing periods from the sample of Yang (2013)

#### 4 CONCLUSIONS

The main results from the light curve solutions of our data are as follows.

- (1) We determined the initial epochs  $T_0$  of the four targets (Table 5).
- (2) We improved the period of NSVS 3853195 (Table 5) on the base of all photometric data: CRTS, NSVS, SWASP and IRIDA. The previous period values of the other three targets fitted well our data.
- (3) Our observations revealed that CSS J015404.1+382805 and NSVS 3853195 are the same star (while VSX identified two stars).
- (4) The components of each target are almost the same in mass, temperature, radius and luminosity (Tables 5-6).
- (5) The stellar components of all targets are of G and K spectral types and they undergo partial eclipses.
- (6) All targets have overcontact configurations with small fillout factor (Fig. 3, Table 6). This means that they probably are newly formed contact binaries (Qian et al. 2014).
- (7) Three binaries revealed O’Connell effect that was reproduced by cool spots (Table 7) on their primary components. They are appearances of the magnetic activity of these targets.
- (8) All our targets have mass ratio  $q \geq 0.88$  (Table 5), i.e. they belong to the H subtype W UMa systems (with  $q \geq 0.72$ ). Csizmadia & Klagyivik (2004) revealed that the different subtypes of W UMa’s are located into different regions on the mass ratio – luminosity ratio diagram (their fig. 1) but above the line  $l_2/l_1 = q^{4.6}$

**Table 8** Parameters of the cool spots of the targets

Star	$q$	$l_2/l_1$	$f$	References
AD Cnc	0.77	1.00	0.08	<a href="#">Qian et al. (2007)</a>
BI Vul	0.97	1.22	0.04	<a href="#">Qian et al. (2013)</a>
CSTAR 038663	0.89	1.13	0.10	<a href="#">Qian et al. (2014)</a>
ISWASP J174310.98+432709.6	1.00	0.65	0.23	<a href="#">Kjurkchieva et al. (2015a)</a>
NSVS 11234970	0.99	0.55	0.21	<a href="#">Kjurkchieva et al. (2015a)</a>
NSVS 11504202	0.98	0.71	0.00	<a href="#">Kjurkchieva et al. (2015a)</a>
NSVS 11534299	0.87	0.77	0.00	<a href="#">Kjurkchieva et al. (2015a)</a>
NSVS 1776195	0.83	0.96	0.00	<a href="#">Kjurkchieva et al. (2015b)</a>
NSVS 113026	0.79	1.00	0.07	<a href="#">Kjurkchieva et al. (2015b)</a>
NSVS 2244206	0.73	0.53	0.26	<a href="#">Kjurkchieva et al. (2016a)</a>
NSVS 908513	0.71	0.60	0.15	<a href="#">Kjurkchieva et al. (2016a)</a>
VSX J062624.4+570907	0.77	0.63	0.16	<a href="#">Kjurkchieva et al. (2016a)</a>
CSS J171508.5+350658	0.89	0.64	0.00	<a href="#">Kjurkchieva et al. (2016b)</a>
USNO-B1.0-1395-0370184	0.97	0.90	0.01	<a href="#">Kjurkchieva et al. (2016c)</a>
USNO-B1.0-1395-0370731	0.85	0.83	0.25	<a href="#">Kjurkchieva et al. (2016c)</a>
NSVS 2459652	0.786	0.73	0.17	<a href="#">Kjurkchieva et al. (2016d)</a>
NSVS 7377875	0.898	0.84	0.11	<a href="#">Kjurkchieva et al. (2016d)</a>
V796 Cep	0.95	0.95	0.10	this paper
V797 Cep	0.89	0.77	0.07	this paper
CSS J015341.9+381641	0.89	0.87	0.17	this paper
NSVS 3853195	0.90	0.86	0.09	this paper

representing the mass-luminosity relation for MS detached stars. Our targets support this conclusion and the relation between their mass ratio and luminosity ratio is  $l_2/l_1 = q^{1.5}$ , i.e. close to that of [Lucy \(1968b\)](#).

(9) The investigation of shallow-contact binary stars with high mass ratios is important for the modern astrophysics because they are considered as newly formed contact configurations, at the beginning of contact evolution ([Qian et al. 2014](#)). The most detailed studies of this type refer to the binaries AD Cnc ([Qian et al. 2007](#)), BI Vul ([Qian et al. 2013](#)) and CSTAR 038663 ([Qian et al. 2014](#)). They revealed that these cool, short-period (0.25–0.28 d), shallow-contact binaries exhibit strong magnetic activity (including optical 0.2 mag flares of CSTAR 038663) and multiple period changes. Recently we observed and modelled (in the same way) shallow-contact W UMa's of H subtype (Table 8). On the diagram fillout factor–mass ratio (Fig. 4) the targets from Table 8 fall into the bottom right (red triangles) due to their small fillout factors (0.0–0.25) and high mass ratios (0.7–1.0). On the same diagram the contact binaries with decreasing periods from the

sample of Yang et al. (2013) constitute cluster (black circles) to the upper-left from our sample because they have intermediate fillout factors (0.05–0.30) and moderate mass ratios (0.3–0.6). One could guess that the deep-contact W UMa's would form a third cluster more left and upwards from the first two clusters on the diagram. So, the diagram fillout factor–mass ratio acquires evolutionary meaning: through the common envelope phase the position of a given star will describe a trace starting from the bottom right and ending to the upper left side of the diagram.

More investigations of shallow-contact binary stars with high mass ratios will provide more statistics of their global parameters and opportunity for further study of the rapid evolution of binary stars reached the contact stage. The presented study is only a step in that direction.

**Acknowledgements** This work was supported partly by grants H08/21 and M08/02 of the Fund for Scientific Research of the Bulgarian Ministry of Education and Science. This publication makes use of data products from the Two Micron All Sky Survey, which is a joint project of the University of Massachusetts and the Infrared Processing and Analysis Center/California Institute of Technology, funded by the National Aeronautics and Space Administration and the National Science Foundation. This research also has made use of the SIMBAD database, operated at CDS, Strasbourg, France, NASA's Astrophysics Data System Abstract Service, the USNOFS Image and Catalogue Archive operated by the United States Naval Observatory, Flagstaff Station (<http://www.nofs.navy.mil/data/fchpix/>) and the photometric software VPHOT operated by the AAVSO, Cambridge, Massachusetts. The research was supported partly by funds of project RD 02-81 of the Shumen University. The authors are grateful to the anonymous referee for the valuable notes and recommendations.

## References

- Berry, R., & Burnell, J. 2006, in *The Handbook of Astronomical Image Processing*, 86
- Binnendijk, L. 1965, in *Veroeffentlichungen der Remeis-Sternwarte zu Bamberg*, Nr. 40, 36
- Csizmadia, S., & Klagyivik, P. 2004, *A & A*, 426, 1001
- Eker, Z., Bilir, S., Yaz, E., Demircan, O., & Helvacı, M. 2009, *AN*, 330, 68
- Gettel, S. J., Geske, M. T., & McKay, T. A. 2006, *AJ*, 131, 621
- Gilliland, R. L., & Brown, T. M. 1988, *PASP*, 100, 754
- Henden, A. 2016, *AAVSO*, 44, 84
- Honeycutt, R. K. 1992, *PASP*, 104, 435
- Ivanova, N., Justham, S., Chen, X., et al. 2013, *A & ARv*, 21, 59

- Kipping, D. M. 2010, MNRAS, 408, 1758
- Kjurkchieva, D. P., Dimitrov, D. P., & Ibryamov, S. I. 2015a, RAA, 15, 1493
- Kjurkchieva, D. P., Popov, V. A., Vasileva, D. L., & Petrov, N. I. 2016a, RAA, 16, 135
- Kjurkchieva, D., Popov, V., Petrov, N., & Ivanov, E. 2015b, CoSka, 45, 28
- Kjurkchieva, D., Popov, V., Vasileva, D., & Petrov, N. 2016b, SerAJ, 192, 21
- Kjurkchieva, D., Popov, V., Vasileva, D., & Petrov, N. 2016c, SerAJ, 193, 27
- Kjurkchieva, D., Popov, V., Vasileva, D., & Petrov, N. 2016d, RevMexAA, in press
- Klagyivik, P., & Csizmadia, S. 2004, in Publications of the Astronomy Department of the Eotvos University, ed. E. Forgacs-Dajka, K. Petrovay, & R. Erdelyi, Vol. 14, 303
- Kwee, K. K., & van Woerden, H. 1956, Bulletin of the Astronomical Institutes of the Netherlands, 12, 327
- Lucy, L. B. 1968a, ApJ, 153, 877
- Lucy, L. B. 1968b, ApJ, 151, 1123
- Martin, E. L., Spruit, H. C., & Tata, R. 2011, A & A, 535, A50
- Prsa, A., & Zwitter, T. 2005, ApJ, 628, 426
- Prsa, A., Conroy, K. E., Horvat, M., et al. 2016, arXiv:1609.08135
- Qian, S. 2003, MNRAS, 342, 1260
- Qian, S.-B., Yuan, J.-Z., Snoonthornthum, B., et al. 2007, ApJ, 671, 811
- Qian, S.-B., Liu, N.-P., Li, K., et al. 2013, ApJS, 209, 13
- Qian, S.-B., Wang, J.-J., Zhu, L.-Y., et al. 2014, ApJS, 212, 4
- Rucinski, S. M. 1994, PASP, 106, 462
- Rucinski, S. M. 2004, NewAR, 48, 703
- Rucinski, S. M., & Duerbeck, H. W. 1997, PASP, 109, 1340
- Stepien, K. 2006, AcA, 56, 199
- Tokunaga, A. T. 2000, in Allen's astrophysical quantities, 4th, ed. A. N. Cox, 143
- van Hamme, W. 1993, AJ, 106, 2096
- Webbink, R. F. 1984, ApJ, 277, 355
- Willems, B., & Kolb, U. 2004, A & A, 419, 1057
- Wilson, R. E. 1979, ApJ, 234, 1054
- Wilson, R. E., & Devinney, E. J. 1971, ApJ, 166, 605
- Yang, Y.-G., Qian, S.-B., & Dai, H.-F. 2013, AJ, 145, 60
- Zacharias, N., Finch, C. T., Girard, T. M., H. A., et al. 2013, AJ, 145, 44